The Nanoscale Architecture of Force-Bearing Focal Adhesions

ARTICLE *in* NANO LETTERS · JULY 2014

Impact Factor: 13.59 · DOI: 10.1021/nl5008773 · Source: PubMed

7 AUTHORS, INCLUDING:

Rolf Harkes
Leiden University
9 PUBLICATIONS **14** CITATIONS
SEE PROFILE

Ewa M Spiesz
Queen Mary, University of London
15 PUBLICATIONS **81** CITATIONS
SEE PROFILE

Danny van Noort
no institute at the moment
59 PUBLICATIONS **1,251** CITATIONS
SEE PROFILE

Benoit Ladoux
Paris Diderot University
75 PUBLICATIONS **3,177** CITATIONS
SEE PROFILE

NANO LETTERS

Letter

pubs.acs.org/NanoLett

The Nanoscale Architecture of Force-Bearing Focal Adhesions

Hedde van Hoorn,[†] Rolf Harkes,[†] Ewa M. Spiesz,[‡] Cornelis Storm,[‡] Danny van Noort,[§] Benoit Ladoux,[§,∥] and Thomas Schmidt*[,†]

[†]Physics of Life Processes, Kamerligh Onnes-Huygens Laboratory, Leiden University, Niels Bohrweg 2, 2333 CA Leiden, The Netherlands

[‡]Department of Applied Physics and Institute for Complex Molecular Systems, Eindhoven University of Technology, P.O. Box 513, 5600 MB Eindhoven, The Netherlands

[§]Mechanobiology Institute (MBI), National University of Singapore (NUS), Engineering Drive 1, Singapore 117411, Singapore

[∥]Institut Jacques Monod, Université Paris Diderot and CNRS UMR 7592, 15 rue Hélène Brion, 75013 Paris, France

Supporting Information

ABSTRACT: The combination of micropillar array technology to measure cellular traction forces with super-resolution imaging allowed us to obtain cellular traction force maps and simultaneously zoom in on individual focal adhesions with single-molecule accuracy. We achieved a force detection precision of 500 pN simultaneously with a mean single-molecule localization precision of 30 nm. Key to the achievement was a two-step etching process that provided an integrated spacer next to the micropillar array that permitted stable and reproducible observation of cells on micropillars within the short working distance of a high-magnification, high numerical aperture objective. In turn, we used the technology to characterize the super-resolved structure of focal adhesions during force exertion. Live-cell imaging on MCF-7 cells demonstrated the applicability of the inverted configuration of the micropillar arrays to dynamics measurements. Forces emanated from a molecular base that was localized on top of the micropillars. What appeared as a single adhesion in conventional microscopy were in fact multiple elongated adhesions emanating from only a small fraction of the adhesion on the micropillar surface. Focal adhesions were elongated in the direction of local cellular force exertion with structural features of 100−280 nm in 3T3 Fibroblasts and MCF-7 cells. The combined measure of nanoscale architecture and force exerted shows a high level of stress accumulation at a single site of adhesion.

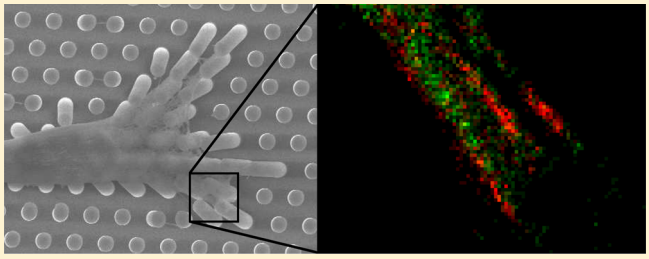

KEYWORDS: *Cell mechanics, mechanobiology, focal adhesion, mechanosensing, super-resolution*

It has come as a surprise recently that cells respond not only to biochemical cues but also to the mechanical properties of their local environment.[1−4] Studies showed the stiffness-dependent differentiation of stem cells,[5] stiffness-directed cell motility (durotaxis),[6] and the importance of the environmental mechanical properties in disease like cancer.[7,8] While these phenomena may have different biological relevance, all start at a common origin: the measurement of the mechanical response of the microenvironment performed by the cell, followed by some unexplored mechanochemical coupling that finally leads to a cellular phenotype.

The cellular structures at which mechanical signals could be measured and analyzed are the focal adhesions (FA). At these sites, the physical connection between the internal contractile cytoskeleton and the extracellular matrix is made through integrin-dimers spanning the cell membrane. On the cytosolic side of the integrins a huge multiprotein complex is formed that attaches to the actin cytoskeleton. The latter forms an active cellular mechanical network contracted by myosin-motor activity. More than 100 proteins have been identified in FAs that define a biological network with a multitude of interactions.[9] Several FA proteins have been suggested to potentially serve as mechanochemical transducers that alter their biochemical function according to the amount of mechanical force exerted. These mechanosensors include talin,[10] vinculin,[11] p130Cas,[12] zyxin,[13] and paxillin.[14] It has been proposed that upon force exertion on those mechanosensors, specific binding sites become available that promote further biochemical interaction. However, it remains unclear whether the FA complex undergoes enough deformation and force exertion to physically stretch such proteins to perform their mechanosensing activity. We should thus examine on what length scale deformations occur and how much force is carried by FA proteins to enable a comparison to in vitro studies. Knowledge about the nanostructured organization of a FA relative to a local site of force exertion has the potential to address these open issues and to provide novel insights about

Received: March 7, 2014
Revised: June 17, 2014

dx.doi.org/10.1021/nl5008773 | *Nano Lett.* XXXX, XXX, XXX−XXX

the physical interpretation of local mechanosensory mechanisms.

The lack of knowledge is in part due to a lack of experimental methodology that permits direct measurement of the locally exerted force and simultaneously quantify the local molecular stoichiometry inside a FA complex. Here, we present methodology that combines two high-resolution optical imaging techniques that enabled us to directly correlate molecular arrangements and cellular forces. In our approach, micropillar array technology was used to quantify sub-nN local cellular forces.[15−17] We show the ability to combine this technique with fixed- and live-cell fluorescence microscopy, giving diffraction limited results comparable to previous work.[18−20] Simultaneously, we employed super-resolution optical microscopy[21−23] with a localization precision of 30 nm to quantify the nanostructure of paxillin and phosphorylated paxillin in focal adhesions.

Prior studies have demonstrated that super-resolution microscopy yields insights into the dynamics and composition of focal adhesion complexes.[24,25] To those super-resolution studies we here add the simultaneous readout of cellular forces at high resolution in an inverted micropillar arrangement. First, we show that inversion of the micropillar array to an upside-down configuration on an optical microscope with high-sensitivity multicolor fluorescence imaging capability allows us to accurately measure whole-cell mechanics in both fixed- and live-cells. Second, we demonstrate that simultaneous super-resolution microscopy allows us to zoom in onto FAs to generate a molecular density map of phosphorylated paxillin stained by antibodies as well as two-color super-resolution on actin and paxillin. Taken together, our approach provides a sub-nN force precision map of cellular force exertion together with a super-resolved paxillin density map that directly measures the nanoscale architecture of force-bearing focal adhesions. Finally, our measurements demonstrate that multiple small, elongated FAs with dimensions of 100−280 nm carry forces of 10−20 nN, which leads to local stress accumulation up to 300 nN/μm^2. Force is thus carried through smaller structures than could be quantified using diffraction-limited microscopy and the diffraction limited stress measured on the same micropillar arrays was an order of magnitude smaller. Quantification of the stress accumulation at a focal adhesion site indeed provides the potential to check whether specific FA proteins can act as mechanosensors.

Results and Discussion. *High-Resolution Measurement of Cellular Forces.* First, we assured that cell behavior on inverted pillar arrays did not differ from cell behavior in upright chambers. Phenomenologically we found that cells showed a healthy morphology, migrated, and divided as expected. We further performed both live-cell and fixed-cell imaging on 3T3 fibroblasts to confer the phenomenological findings. We found that force exertion evolved from the cell periphery, and was largely aligned with actin stress fibers (Figure 2A). After careful calibration of the micropillars using finite-element analysis (see Supporting Information), the total vectorial force per cell was zero within experimental uncertainty. The absolute force per pillar in each cell varied over a large range from 0 to 10 nN (Figure 2B) with a mean of 4 ± 3 nN (mean ± std). Typically, most of the large forces were localized on a few (5−10) pillars per cell.

Multicolor imaging of paxillin and actin confirmed that cellular forces emerged from FAs with their edges attached to the top of the pillars as shown in Figure 2A,B (Supporting

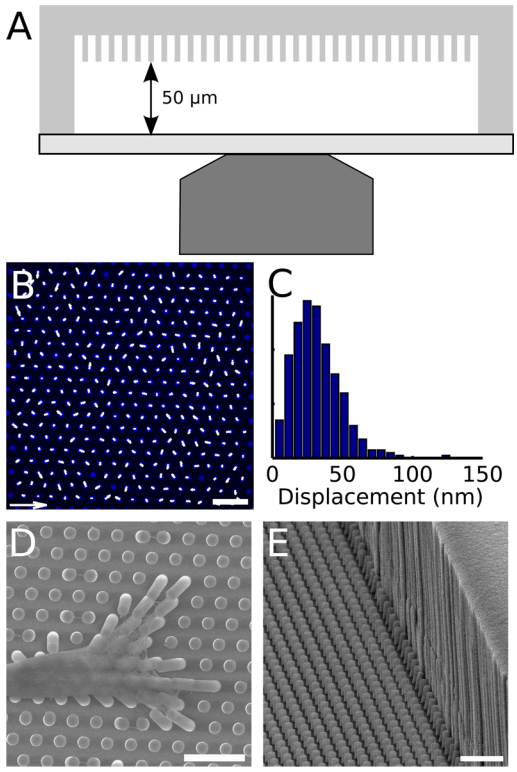

Figure 1. Inverted micropillars with well-defined spacers provide simultaneous super-resolution fluorescence- and force measurements. (A) Schematic overview of configuration during microscopy (not to scale). With a 100 μm coverslip and 50 μm spacer next to the array, micropillars and cells are within working distance of a high-NA objective. (B) A fluorescence image of the micropillars is analyzed to show the resolution of the deflection field (scalebar in lower left is for the pillar deflections corresponding to 500 nm, lower right is for the fluorescence image corresponding to 10 μm). (C) Histogram of the absolute deflections in (B) shows a mean deflection of 30 nm, giving the one-dimensional localization precision. (D) Scanning electron microscopy (SEM) of a 3T3 fibroblast spread on a micropillar array shows deflected pillars. (E) One 50 μm high spacer, as seen with SEM, flanking the micropillar array. (Scalebars in D,E correspond to 10 μm.)

Information Figure 2 shows separate channels and a z-stack is shown in Supporting Information movie 2). The FAs were detected by an antibody that recognizes phosphorylated paxillin. The focal adhesion area was distributed between 0.5 to 3 μm^2 with a mean of (1.4 ± 0.7) μm^2 (Figure 2C). Larger-sized FAs were able to support larger forces as indicated by the correlation between FA area and force displayed in Figure 2C. Assuming a linear relationship the local force increased by (3 ± 1) nN/μm^2 of FA area. A similar range of forces and FA area was previously found for Human Foreskin Fibroblasts[18] and REF52 Fibroblasts.[19]

Shapes and sizes of FAs were quantified using custom software to detect the edges of focal adhesions (Supporting Information Figure 3). Those quantities were correlated to local cellular traction forces. Actin stress fibers (mostly cortical fibers) were formed throughout the cell and emerged from force-bearing FAs (Figures 2A,B). Throughout all cells, we observed a homogeneous distribution of orientation for both forces and focal adhesion elongation. This was predicted because there is no preferential orientation for cells on hexagonal pillar arrays. However, we found a clear correlation between the direction of force and the direction of FA

dx.doi.org/10.1021/nl5008773 | Nano Lett. XXXX, XXX, XXX−XXX

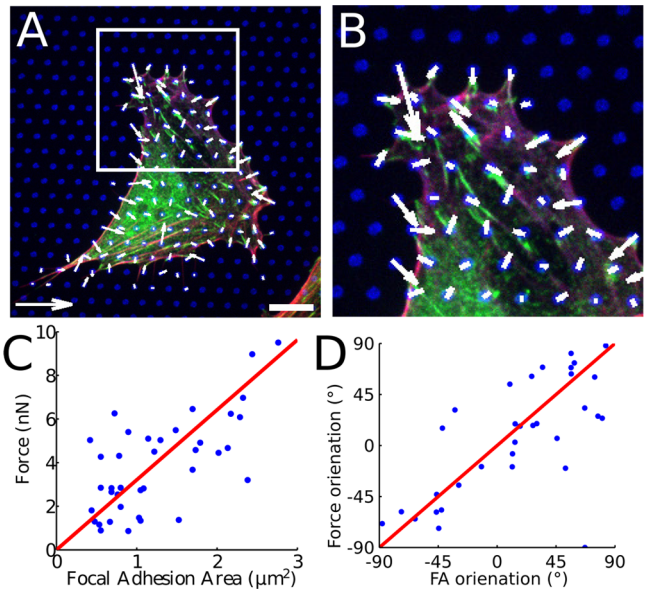

Figure 2. Force exertion is guided from actin stress fibers through focal adhesions. (A) 3T3 fibroblast on hexagonal pillar array microcontact printed with fibronectin (blue), immunostained for paxillin (green) and actin (red) and (B) zoomed in on forces exerted with focal adhesions and actin (in A lower left arrow scalebar corresponds to 20 nN force, lower right scalebar corresponds to 10 μm). (C) The force exerted locally increases with focal adhesions size, a fit to the data gives (3 ± 1) nN/ μm^2 (R^2 = 0.459). (D) Focal adhesions co-orient with the direction in which the force is exerted, a correlation of 1 deg/deg is shown in red (a histogram of the co-orientation gives a standard deviation of 10° around a mean difference in orientation of 0°).

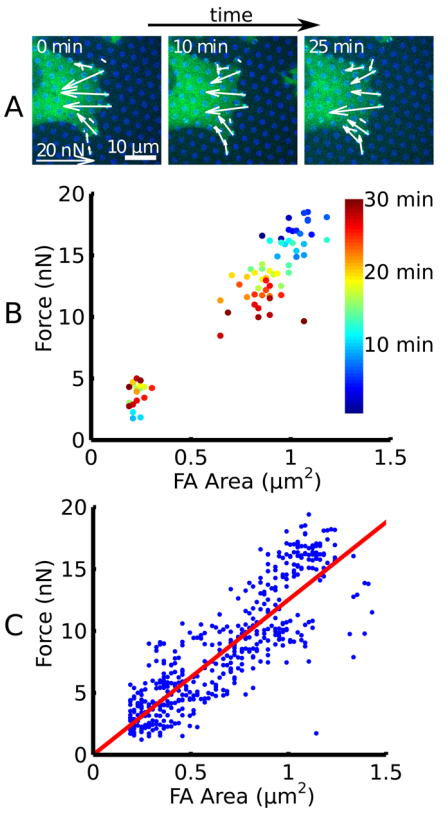

Figure 3. Live-cell dynamics of focal adhesions and force. (A) Live MCF-7 cell expressing paxillin-GFP on a micropillar array exerts significant forces locally where FAs are present. (B) Force and FA area correlate over time from two individual pillar locations. Color correlates to time, indicating FA and force decrease for one pillar, while another grows in force at a constant small FA size. (C) Over multiple focal adhesions and sites of force exertion on live MCF-7 cells, a clear correlation is given by a linear fit with (13 ± 2) nN/μm^2 (R^2 = 0.711).

elongation. FAs were oriented within 10° (standard deviation) with respect to the direction of force (Figure 2D).

Live-cell imaging of FAs in MCF-7 cells stably expressing a paxillin-GFP fusion construct in the inverted configuration further confirmed the ability to perform live-cell experiments in the inverted configuration and local force-FA area correlations. In Figure 3A, snapshots of a migrating cell on micropillars (blue) expressing paxillin-GFP (green) are shown (Supporting Information movie 3 shows live-cell dynamics). FA dynamics were directly quantified. The local FA area followed the force again in an apparent linear relationship (quantification of the FAs over time is shown in Supporting Information movie 4). For two individual pillars (Figure 3B) force and FA area correlated over time as one decreased in force and FA area and the other increased in force at an approximately constant small FA area. The force in live-cell experiments increased with FA area with (13 ± 2) nN/μm^2 (Figure 3C).

Our measurements of FA characteristics, cellular forces, and their correlations corroborate previous observations of fibroblast-behavior when grown in the upright configuration.[18−20] Using our inverted approach we can furthermore characterize live-cell force and FA area dynamics at the highest possible diffraction-limited resolution. Hence, we conclude that cells that are spread on inverted pillar arrays remain viable and their phenotypic and mechanical behavior is unaltered with repect to other situations.

Super-Resolved Imaging of Focal-Adhesion Proteins on Micropillar Arrays. In order to relate cellular forces to the molecular structure of focal adhesion complexes, we performed super-resolution imaging of the FA protein paxillin in cells that pulled on micropillar arrays.[23] After adhesion, cells were fixed and immunostained for phosphorylated paxillin (pY118) using the primary rabbit-anti-pY118 Paxillin antibody. Subsequently, a secondary Alexa647-antirabbit antibody was used for fluorescence-labeling. Cells were imaged in phosphate-buffered saline at pH 8 supplemented with 100 mM mercapto-ethylamine and a glucose-oxidase oxygen-scavenging system (for details see Supporting Information). After prebleach, Alexa647 was reactivated with 405 nm light for 10 ms every 20 frames with increasing intensity (1−20 W/cm^2) such that a constant 10 to 20 Alexa647 molecules were observed in each image. Individual Alexa647 molecules were identified and localized when excited at 642 nm for 10 ms with an intensity of 1.5 kW/cm^2 (see Supporting Information movie 1 for raw data). In total, 15,000 images were recorded within 5 min. From those data we reconstructed a super-resolved image of FAs on pillars with a mean one-dimensional localization-precision of 30 nm. Figure 3A exemplifies the largely increased resolution of the super-resolved image (right) in comparison to the image taken at diffraction-limited resolution (left, the full diffraction-limited image is depicted in Supporting Information Figure 4). Note the scalebar of 2 μm in this image when comparing to the image in Figure 2B. FAs that appear as elliptical globular structures in the diffraction-limited images

dx.doi.org/10.1021/nl5008773 | *Nano Lett.* XXXX, XXX, XXX−XXX

(Figure 2B) appear rather as elongated stretches of width 100−500 nm and length 1−5 μm in the super-resolved image.

Labeling the micropillars with Alexa405-fibronectin allowed us to overlay the super-resolution images of FAs with diffraction-limited images of the micropillar arrays resulting in high-resolution force-maps. Figure 4B shows such overlay in

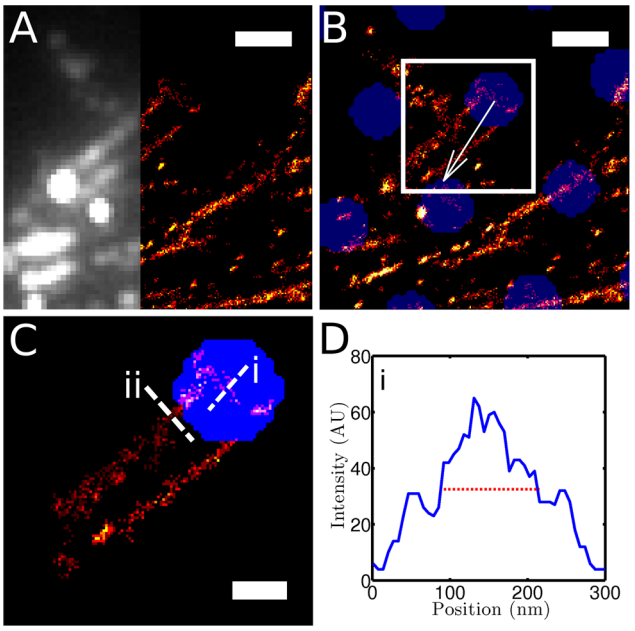

Figure 4. Nanoscale architecture of force bearing focal adhesions. (A) Super-resolved structure of phosphorylated paxillin using dSTORM. The diffraction limited image (left side) cannot resolve the small structural features of focal adhesions, but the super-resolved image (right side) reveals smaller features. (B) Micropillar locations are correlated to the super-resolved FAs through direct observation of the Alexa405-labeled fibronectin in blue during dSTORM reactivation. The arrow corresponds to a force of 6.5 nN. (C) A closer look at a single site of force exertion reveals a super-resolved image of a force-bearing FA (scalebars in A,B correspond to 2 μm and in C to 1 μm). (D) Collapsed histogram of multiple line profiles along the FA base, as denoted by i in C. The base of the elongated FAs is only 125 nm wide and is perpendicular to two elongated FA structures.

which the pillar indicated by an arrow was deflected significantly with a force of 6.5 nN, which is carried by two individual elongated FAs. From such images, it becomes obvious that the cell's major forces emerge from elongated FAs that end on pillars, and that FA elongation is parallel to force exertion (as we observed in Figure 2D). However, in the super-resolved image the attachment region of FAs to fibronectin is more clearly resolved. The FA is elongated but also clearly localized on the very top of the pillars. Furthermore, we observe that the FA cluster extends several micrometers beyond the pillar. Fibroblasts produce fibronectin by which they model a fibrous network left behind when cells move forward (staining for fibronectin is shown in Supporting Information Figure 5). The elongated FA in Figure 4B attached to fibronectin left behind by the cell leading to the elongated growth of FAs toward the cell center.

With super-resolved imaging, we further characterized the nanoscale architecture of the focal adhesions bearing the force exerted on a single pillar, as exemplified in Figure 4C. In this case, two focal adhesions emerged in parallel at a distance of 1 μm and carried a force of 6.5 nN. The two parallel focal adhesions each measured a width of 280 nm at the full width of half-maximum (fwhm, see Supporting Information Figure 6). Strikingly, the base of contact in Figure 4C on top of the pillar shows an additional structure 125 nm wide (fwhm, Figure 4D) perpendicular to the two elongated FAs. In all super-resolution images analyzed, we found that force-exertion clearly emerged from the top of the pillars and from localized FA structures that had a width of 125−280 nm fwhm for 3T3 fibroblasts.

We also examined the super-resolved structure of paxillin in the MCF-7 cells used for live-cell microscopy (see Figure 3). Directly labeled Alexa647-nanobodies recognizing the beta-barrel of GFP on the paxillin and Alexa532-labeled phalloidin were used to reconstruct a two-color super-resolution image (see Figure 5). The structure of the FAs (Figure 5A) appeared similar to what we obtained from super-resolved phosphorylated paxillin in Figure 4C. Actin bundles preceded the elongated FAs carrying the exerted force (Figure 5B). Again, multiple elongated stretches emanated from the top of the micropillars bearing forces in the order of 0−20 nN (zoom in on a single pillar in Figure 5C) with a width of 100−150 nm.

With the super-resolved structure of FAs carrying a local force, we measured the FA area more accurately as compared to diffraction-limited microscopy. For both cell types, it was apparent that the local force exerted was distributed over small FAs, consisting of multiple elongated 100−280 nm wide stretches. From these smaller FA areas, the actual force per area amounted to 10−300 nN/μm^2. The stress accumulated is thus approximately 1 order of magnitude higher as compared to the values we and others[18−20] obtained using diffraction-limited experiments. The individual sites of attachment as in the

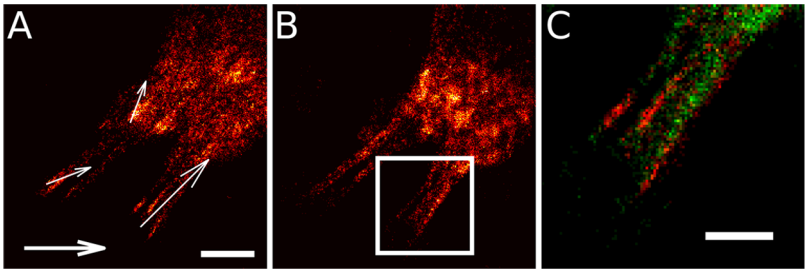

Figure 5. Super-resolved focal adhesions and actin correlated to force. Fixed MCF-7 cells show super-resolved paxillin using Alexa647-nanobody staining directly to paxillin-GFP and Alexa532-phalloidin to actin. (A) Paxillin molecular density and (B) actin molecular density through dSTORM imaging relative to force exertion. (C) A closer look at the location of one pillar shows multiple elongated FAs that emanate into actin bundles with a width of 100−150 nm. (Scalebars in A, also valid for B: lower-left corresponds to 20 nN and lower-right to 2 μm. Scalebar in C corresponds to 1 μm).

dx.doi.org/10.1021/nl5008773 | *Nano Lett.* XXXX, XXX, XXX−XXX

enlargement in Figure 5C thus carried an even larger force per FA area, making it a locally highly stress-bearing state.

Conclusion. With one additional step in the micropillar fabrication procedure, we achieved simultaneous high-resolution cellular traction force measurements and super-resolution imaging. The precisely fabricated and integrated spacers next to the microfabricated pillar array allowed us to perform microscopy using high-NA objectives that are required for super-resolution microscopy. With our approach, it became possible to measure local focal adhesion molecule-densities and the local force exerted by the cell at the same location. The ability to perform super-resolution measurements further makes our approach an attractive technique to address the question of a global versus local mechanosensory mechanism.

Cells that were attached on inverted micropillar arrays remained viable, as observed by proliferation and mechanical characteristics. Cellular force maps with high resolution down to the sub-nN force precision were obtained for fixed 3T3 fibroblasts and live MCF-7 cells. Simultaneously, we were able to image the nanostructural organization of the focal adhesion protein paxillin. Our method further allowed us to characterize exact adhesion size and localization relative to forces. Focal adhesions in 3T3 fibroblasts and in MCF-7 cells were elongated parallel to the direction of force exertion and had a typical width of 100−280 nm. The approximate stress carried by a FA complex was 1 order of magnitude higher as compared to the diffraction-limited case, since the FA actually consisted of multiple narrow elongated structures. Our measurements thus revealed a higher stress accumulation compared to previous measurements on cellular adhesion sites.

With the ongoing developments to quantify the exact number of molecules in super-resolution imaging,[26] our approach can be directly used to quantify the amount of specific force-bearing molecules in a FA. We estimated that the focal adhesion structures localized on the pillar presented in Figure 4C contained about 780 paxillin molecules. Combined with the measure of the local force we may in the future be able to complete our image of how forces are transmitted through the multifaceted focal adhesion complex. It will be interesting to investigate, using our methodology, the structure-force responses of potential mechanosensory proteins like talin, vinculin, p130Cas, and zyxin. Such experiments may shed light on how a cell structurally alters its adhesion organization depending on its mechanical behavior.

Methods. *Cell Biology.* The 3T3 fibroblasts were cultured in high-glucose Dulbecco's Modified Eagle's Medium (DMEM) supplemented with 10% calf serum (Thermo Scientific), 2 mM glutamine, and 100 μg/mL pennicilin/streptomycin. MCF-7 cells stably expressing a paxillin-GFP fusion construct (a gift from Erik Danen at Leiden University) were cultured in DMEM supplemented with 10% fetal calf serum (Thermo Scientific), 2 mM glutamine, and 100 μg/mL pennicilin/streptomycin. Cells were seeded at single cell density directly on the micropillar array. Cells were allowed to spread for 8 to 24 h. Micropillar arrays were subsequently inverted onto #0, 25 mm diameter, round coverslips (Menzel Glaser). The micropillar arrays were kept from floating using a support weight of glass. Live-cell measurements were performed in overnight time-lapse measurements on a confocal spinning-disk setup with a home-built focus-hold system. The temperature was kept at 37 °C with constant 5% CO2 concentration in a stage-top incubator (Tokai Hit, Japan). Cells were fixed in 4% paraformaldehyde 16−24 h after seeding for immunolabeling.

Confocal Microscopy. All diffraction-limited fixed and live-cell imaging was performed on a home-built setup based on an Axiovert200 microscope body (Zeiss). An in-house focus-hold system performing feedback on the reflected light from a 850 nm laser-diode at the glass−water interface assured overnight experiments with axial drift <1 μm. Confocal imaging was achieved by means of a spinning disk unit (CSU-X1, Yokogawa). The confocal image was acquired on an emCCD camera (iXon 897, Andor). IQ-software (Andor) was used for basic setup-control and data acquisition. Specifically developed software (Labview, National Instruments) controlled the autofocus and automated XY positioning (Marzhauser XY-stage). Illumination was performed with five different lasers of wavelength 405, 488, 514, 561, and 642 nm (CrystaLaser, Coherent, Cobolt (2×) and Spectra Physics, respectively). Accurately controlled excitation intensity and excitation timing was achieved using an acousto-optic tunable filter (AA Optoelectronics). Light was coupled into the confocal spinning-disk unit by means of a polarization maintaining single-mode fiber.

Force Measurement on Micropillar Arrays. A hexagonal array of poly dimethyl-siloxane (PDMS, Sylgard 184, Dow Corning) micropillars of 2 μm diameter, 2 μm spacing, and with a height of 6.9 μm were produced using replica-molding from a silicon wafer into which the negative of the structure was etched by deep reactive-ion etching (for details see Supporting Information). The pillar arrays were flanked by integrated 50 μm high spacers (shown in Figure 1A,E) such that pillar tops and hence cells attaching to them were within the limited working distance of a high-NA objective (<170 μm) on an inverted microscope. The use of a high-NA objective is a prerequisite for any high-resolution optical imaging. Further, such objectives provide the high collection-efficiency which is essential to super-resolution imaging.

The tops of the micropillars were coated with a mixture of Alexa405-labeled and unlabeled fibronectin (1:5) using micro-contact printing. This approach ensured that cells were solely attached to the tops of the micropillars as confirmed by confocal microscopy (data not shown). Finite element analysis that was fed the exact micropillar dimensions (Supporting Information Figure 1) as measured by in situ scanning electron microscopy (SEM, FEI nanoSEM) allowed us to precisely calibrate the force-deflection relation (for details see Supporting Information). Pillars on the array had a characteristic spring constant of 16.7 nN/μm. The position of the pillar tops was observed by fluorescence microscopy at 405 nm excitation. From those fluorescence images (Figure 1B, pillar array without cells) the exact pillar-centroid positions were determined down to 30 nm accuracy using specifically designed software (Matlab, Mathworks). The deflection precision of 30 nm, that is solely limited by the fluorescence signal from an individual pillar, corresponded to a force accuracy of 500 pN (Figure 1C).

Experimental results were presented with at least three independent experiments per graphical representation, performed on at least four different cells per experiment. When fitting was performed to results, R^2 analysis gives the accuracy of the fit. An example of a fixed and dehydrated cell on pillars when imaged in a low-vacuum mode SEM is shown in Figure 1D. It should be noted that the deflections of the pillars in this image are larger than in live-cell measurements due to the dehydration procedure needed for electron-microscopy.

Super-Resolution Imaging on Micropillar Arrays. The upside-down micropillar approach with integrated spacers and

dx.doi.org/10.1021/nl5008773 | *Nano Lett.* XXXX, XXX, XXX−XXX

high-NA fluorescence imaging on an inverted microscope allowed us to combine force measurements with super-resolution imaging (for details see Supporting Information). In brief, we labeled paxillin-GFP in the MCF-7 cells with Alexa647-labeled GFP-traps (Chromotek) and phosphorylated paxillin with Alexa647-labeled antirabbit antibody (donkey-antirabbit, Jackson Immunoresearch) to recognize the primary paxillin pY118 antibody (Invitrogen). Alexa647 was reported to show favorable switching properties to employ direct STochastic Optical Reconstruction Microscopy (dSTORM).[23]

Imaging was performed in 100 mM mercaptoethylamine (MEA, Sigma-Aldrich) and a glucose oxygen scavenging system (for details see Supporting Information). By sequential reactivation with 405 nm light from a diode laser (Crystalasers) at 1−20 W/cm^2 and imaging with 642 nm light from a diode laser (Spectra Physics) at 1.5 kW/cm^2, we localized individual molecules to a precision of 30 nm, limited by the signal from an individual molecule of 630 counts per 10 ms of illumination (see Supporting Information movie 1). For simultaneous two-color imaging of the actin structure, we stained with Alexa532-Phalloidin (Invitrogen) and adapted the buffer conditions by removing the oxygen-scavenging system to facilitate favorable switching conditions for Alexa532. The 405 nm switching light also excited the Alexa405-labeled fibronectin on the pillar tops, such that we simultaneously obtained high-resolution information on local cellular forces with each activation step. The combined single-molecule and micropillar approach yielded both a molecular density map of focal adhesion proteins and the local forces exerted by the cell.

■ ASSOCIATED CONTENT

Supporting Information

Experimental procedures, additional figures, and movies of raw data acquiring a super-resolved image, a z-stack from a 3T3 Fibroblast, live MCF-7 cell expressing paxillin-GFP on micropillars, and the same cell analyzed with FA-detection. This material is available free of charge via the Internet at http://pubs.acs.org.

■ AUTHOR INFORMATION

Corresponding Author

*E-mail: schmidt@physics.leidenuniv.nl.

Present Address

(E.M.S.) Queen Mary University of London, U.K.
(D.v.N.) Griffith University, Australia.

Notes

The authors declare no competing financial interest.

■ ACKNOWLEDGMENTS

The authors are grateful for an introduction to the micropillar fabrication technique during a visit at the Mechanobiology Institute in Singapore. Specifically, Man Chun Leong and Sri Ram Krishna Vedula are thanked for their help. Assistance with the tensile testing by Kasper Jansen and Ton Riemslag from TU Delft is gratefully acknowledged. The authors would also like to thank Emrah Balcioglu and Erik Danen of the department of Toxicology at Leiden University for the stable MCF-7 paxillin-GFP cell line, helpful comments and discussions. B.L. acknowledges the Institut Universitaire de France (IUF) for its support. This work was supported by funds from the Mechanobiology Institute (Singapore) and The Netherlands Organization for Scientific Research (NWO-FOM) within the program on Mechanosensing and Mechanotransduction by Cells (FOM L1712M).

■ REFERENCES

(1) Discher, D. E.; Janmey, P.; Wang, Y. L. *Science (New York, N.Y.)* **2005**, *310*, 1139−1143.
(2) Vogel, V.; Sheetz, M. *Nat. Rev. Mol. Cell Biol.* **2006**, *7*, 265−275.
(3) Geiger, B.; Spatz, J. P.; Bershadsky, A. D. *Nat. Rev. Mol. Cell Biol.* **2009**, *10*, 21−33.
(4) Swift, J.; Ivanovska, I. L.; Buxboim, A.; Harada, T.; Dingal, P.; Pinter, J.; Pajerowski, J.; Spinler, K. R.; Shin, J. W.; Tewari, M.; Rehfeldt, F.; Speicher, D. W.; Discher, D. E. *Science (New York, N.Y.)* **2013**, *341*, 1240104.
(5) Engler, A. J.; Sen, S.; Sweeney, H.; Discher, D. E. *Cell* **2006**, *126*, 677−689.
(6) Sochol, R. D.; Higa, A. T.; Janairo, R. R. R.; Li, S.; Lin, L. *Soft Matter* **2011**, *7*, 4606−4609.
(7) C, D. C.; Paszek, M. J.; Weaver, V. M. *Nat. Rev. Mol. Cell Biol.* **2011**, *12*, 308−319.
(8) Swartz, M. A.; Lund, A. W. *Nat. Rev. Cancer* **2012**, *12*, 210−219.
(9) Zaidel-Bar, R.; Itzkovitz, S.; Ma'ayan, A.; Iyengar, R.; Geiger, B. *Nat. Cell Biol.* **2007**, *9*, 858−867.
(10) Margadant, F.; Chew, L. L.; Hu, X.; Yu, H.; Bate, N.; Zhang, X.; Sheetz, M. *PLoS biology* **2011**, *9*, e1001223.
(11) Grashoff, C.; Hoffman, B. D.; Brenner, M. D.; Zhou, R.; Parsons, M.; Yang, M. T.; A, M. M.; Sligar, S. G.; Chen, C. S.; Ha, T.; Schwartz, M. A. *Nature* **2010**, *466*, 263−266.
(12) Sawada, Y.; Tamada, M.; J, D. B.; Cherniavskaya, O.; Sakai, R.; Tanaka, S.; Sheetz, M. P. *Cell* **2006**, *127*, 1015−1026.
(13) Colombelli, J.; Besser, A.; Kress, H.; Reynaud, E. G.; Girard, P.; Caussinus, E.; Haselmann, U.; Small, J. V.; Schwarz, U. S.; Stelzer, E. H. K. *J. Cell Sci.* **2009**, *122*, 1928.
(14) Ronen, Z.; Milo, R.; Kam, Z.; Geiger, B. *J. Cell Sci.* **2007**, *120*, 137−148.
(15) Tan, J. L.; Tien, J.; Pirone, D. M.; Gray, D. S.; Bhadriraju, K.; Chen, C. S. *Proc. Natl. Acad. Sci. U.S.A.* **2003**, *100*, 1484−1489.
(16) du Roure, O.; Saez, A.; Buguin, A.; Austin, R. H.; Chavrier, P.; Silberzan, P.; Siberzan, P.; Ladoux, B. *Proc. Natl. Acad. Sci. U.S.A.* **2005**, *102*, 2390−2395.
(17) Fu, J.; Wang, Y. K.; Yang, M. T.; Desai, R. A.; Yu, X.; Liu, Z.; Chen, C. S. *Nat. Methods* **2010**, *7*, 733−736.
(18) Balaban, N.; Schwarz, U.; Riveline, D.; Goichberg, P.; Tzur, G.; Sabanay, I.; Mahalu, D.; Safran, S.; Bershadsky, A.; Addadi, L.; Geiger, B. *Nat. Cell Biol.* **2001**, *3*, 466−472.
(19) Trichet, L.; Le Digabel, J.; Hawkins, R. J.; Vedula, S. R.; Gupta, M.; Ribrault, C.; Hersen, P.; Voituriez, R.; Ladoux, B. *Proc. Natl. Acad. Sci. U.S.A.* **2012**, *109*, 6933−6938.
(20) Han, S. J.; Bielawski, K. S.; Ting, L. H.; Rodriguez, M. L.; Sniadecki, N. J. *Biophys. J.* **2012**, *103*, 640−648.
(21) Rust, M. J.; Bates, M.; Zhuang, X. *Nat. Methods* **2006**, *3*, 793−795.
(22) Huang, B.; Wang, W.; Bates, M.; Zhuang, X. *Science (New York, N.Y.)* **2008**, *319*, 810−813.
(23) van de Linde, S.; Loschberger, A.; Klein, T.; Heidbreder, M.; Wolter, S.; Heilemann, M.; Sauer, M. *Nat. Protoc.* **2011**, *6*, 991−991009.
(24) Rossier, O.; Octeau, V.; Sibarita, J. B.; Leduc, C.; Tessier, B.; Nair, D.; Gatterdam, V.; Destaing, O.; Corinne, A.; Tampé, R.; Cognet, L.; Choquet, D.; Lounis, B.; Giannone, G. *Nat. Cell Biol.* **2012**, *14*, 1057−1067.
(25) Kanchanawong, P.; Shtengel, G.; Pasapera, A. M.; Ramko, E. B.; Davidson, M. W.; Hess, H. F.; Waterman, C. M. *Nature* **2010**, *468*, 580−584.
(26) Annibale, P.; Vanni, S.; Scarselli, M.; Rothlisberger, U.; Radenovic, A. *Nat. Methods* **2011**, *8*, 527−528.